Nuclear vasohibin-2 promotes cell proliferation by inducing G_0/G_1 to S phase progression

QIANQIAN GE[1*], JIA ZHOU[4*], MIN TU[1*], XIAOFENG XUE[2], ZHANJUN LI[1], ZIPENG LU[1], JISHU WEI[1], GUOXIN SONG[3], JIANMIN CHEN[1], FENG GUO[1], KUIRONG JIANG[1], YI MIAO[1] and WENTAO GAO[1]

[1]Pancreas Center, The First Affiliated Hospital of Nanjing Medical University, Nanjing, Jiangsu; [2]Department of General Surgery, The First Affiliated Hospital of Suzhou University, Suzhou; [3]Department of Pathology, The First Affiliated Hospital, Nanjing Medical University; [4]The First Clinical Medical College, Nanjing Medical University, Nanjing, Jiangsu, P.R. China

Received March 30, 2015; Accepted June 15, 2015

DOI: 10.3892/or.2015.4127

Abstract. As a member of the *vasohibin* (*VASH2*) family, VASH2 is localized intracellularly as a nuclear and cytoplasmic type. Cytoplasmic VASH2 is associated with carcinoma angiogenesis and malignant transformation and promotes cancer growth. However, the function of nuclear VASH2 has yet to be investigated. The aim of the present study was to detect the nuclear VASH2 expression profile in human organs and tissues by protein microarray technique. To examine the function of nuclear VASH2, we analyzed the relationship between nuclear VASH2 and Ki-67, and stably constructed VASH2 overexpression and knockdown in LO2 and HepG2 cell lines, based on a previous study in hepatic cells. The study was conducted using bromodeoxyuridine, immunofluorescent staining, western blot analysis and flow cytometry. Nuclear VASH2 was highly expressed in actively dividing cells in normal and cancer tissues. There was a significant positive correlation between nuclear VASH2 and Ki-67, indicating that nuclear VASH2 positively correlated with cell proliferation in normal and cancer tissues. The bromodeoxyuridine (BrdU) proliferation test showed that nuclear VASH2 increased the S-phase population and promoted cell proliferation, while VASH2 knockdown reduced BrdU absorbance. Cell cycle analysis revealed that nuclear VASH2 overexpression increased the S-phase population in LO2 and HepG2 cells, while nuclear VASH2 knockdown reduced the S-phase population and increased the G_0/G_1 population. The findings of this study challenge the classic view of VASH2, which was previously reported as an angiogenesis factor. Furthermore, to the best of our knowledge, these results are the first clinical data indicating that nuclear VASH2, but not cytoplasmic VASH2, promotes cell proliferation by driving the cell cycle from the G_0/G_1 to S phase.

Correspondence to: Professor Yi Miao or Professor Wentao Gao, Pancreas Center, The First Affiliated Hospital of Nanjing Medical University, 300 Guangzhou Road, Nanjing, Jiangsu 210029, P.R. China
E-mail: miaoyi@njmu.edu.cn
E-mail: gao11@hotmail.com

*Contributed equally

Key words: vasohibin-2, immunohistochemistry, cell proliferation, cell cycle

Introduction

Vasohibin-2 (VASH2) belongs to the VASH family, which also includes VASH1 (1). VASH2 has been identified as a vascular endothelial growth factor (VEGF)-independent angiogenic factor and is expressed preferentially in mononuclear cells that are mobilized from the bone marrow (1,2). Initial analysis of VASH2 revealed that it is also present in endothelial cells (ECs) in developing human or mouse embryos and that its levels are reduced after birth (3). It was reported that VASH2 is transcriptionally activated in human tumors, promoting angiogenesis and growth in hepatic, ovarian and endometrial carcinoma (4-6). VASH2 has shown a strong and extensive ability to promote tumor by epithelial-mesenchymal transition (EMT), increase the proportion of stem cells and inhibit apoptosis, which beyond paracrine promotes angiogenesis and migration (7,8). VASH2 knockdown in cancer cells prominently inhibits growth and angiogenesis in tumors (9). Furthermore, *VASH2* is perceived as a cancer-promoting gene.

However, there are no reliable protein expression studies of VASH2 in human tissue (3). Recently, rabbit anti-human VASH2 polyclonal antibodies were successfully generated for use in western blot analysis (WB) and immunohistochemistry (IHC) (10). It was also determined that, different VASH2 isoforms have different intracellular localizations in HepG2 cells: one (311 amino acids) in the nucleus and the other (355 amino acids) in the cytoplasm (10). According to these differing locations, VASH2 was classified as nuclear and cytoplasmic type (10). Thus, differing locations of VASH2 may have different mechanisms of cell growth promotion. Previous studies have focused on full-length VASH2 (4-9), without a clear distinction between cytoplasmic and nuclear VASH2. In the present study, we focused on nuclear VASH2.

Nuclear VASH2 expression was screened using IHC in human normal and cancer tissues and nuclear VASH2 was found to correlate positively with cell proliferation. The proportion of nuclear VASH2 positivity was positively correlated with the Ki-67-positive proportion in the normal and cancer tissues. Based on these findings, we hypothesized that nuclear VASH2 may be partially involved in the yet unknown mechanisms of cell proliferation. To confirm whether VASH2 is involved in cell proliferation, we stably constructed VASH2 overexpression and knockdown in LO2 and HepG2 cell lines. Cell proliferation was increased in nuclear VASH2-overexpressed cells and decreased in VASH2 knockdown cells. Nuclear VASH2 overexpression promoted G_0/G_1 to S phase progression, while VASH2 knockdown induced upregulation of the G_0/G_1 population. As far as we know, this is the first study to show that nuclear VASH2 promotes cell proliferation by inducing G_0/G_1 to S phase progression. The present study provides a better understanding of the function of VASH2.

Materials and methods

Tissue microarray and IHC. High-density, multiple organ tumors and normal tissue microarray (MC5003a) and multiple organ normal tissue microarrays (FDA999b) were purchased from Biomax (Rockville, MD, USA) for IHC. Squamous epithelial, adjacent non-tumor liver and hepatic cancer tissues were obtained from patients at the First Affiliated Hospital of Nanjing Medical University (Nanjing, China). Written informed consent was obtained from all the patients. The Research Ethics Committee of Nanjing Medical University approved the present study. Primary antibodies used in the present study were as described previously (10): rabbit polyclonal anti-VASH2 (self-prepared) and rabbit polyclonal anti-Ki-67 (Fuzhou Maixin Biotechnology, Fuzhou, China). Ki-67 and nuclear VASH2 staining were evaluated by calculating the proportion of positively stained cells: One thousand cells were counted in each of the 10 randomly selected high-power fields.

Cell culture. The L02 cells were kindly provided by Professor Beicheng Sun of the Department of General Surgery, The First Affiliated Hospital of Nanjing Medical University (Jiangsu, China). Human HepG2 liver cancer cells were obtained from the American Type Culture Collection (ATCC; Manassas, VA, USA). The cells were cultured in Dulbecco's modified Eagle's medium (DMEM) containing 10% fetal bovine serum (FBS) (both from Wisent, QC, Canada) and 100 mg/ml penicillin and 100 mg/ml streptomycin (HyClone, Logan, UT, USA) at 37˚C in 5% CO_2.

Plasmid construction and lentivirus packaging. The highly expressed VASH2 (355 amino acid residues) plasmid fused with the DDK tag at the c-terminal was constructed as previously described (15). VASH2 cDNA (encoding for 311 amino acid residues) purchased from Origene (Rockville, MD, USA) was fused with V5 tag at the c-terminal and cloned into the Lv-CMV-EGFP vector. The plasmids were verified by sequencing (Invitrogen, Shanghai, China). Lentiviral (Lv) constructs were designed to induce nuclear VASH2 overexpression and knockdown, as previously described (4,10). The primer pair for the VASH2 plasmid (311 amino acid residues) was as follows: forward, 5'-CGGCTAGCCCCACCATGACCGGCTC-3' and reverse, 5'-AACTGCAGCTACGTAGAATCGAGACCGAGGAGAGGGTTAGGGATAGGCTTACCAATTCGGATTTGATAGCCCACTT-3' (V5-tag) (10). LO2 and HepG2 cells were stably transfected with Lv-cytomegalovirus (CMV)-VASH2 for VASH2 overexpression (encoding for 311 amino acid residues) and designated as LO2-VASH2 and HepG2-VASH2, respectively. LO2 and HepG2 cells stably transfected with Lv-CMV-EGFP (enhanced green fluorescent protein) as controls were designated as LO2-EGFP and HepG2-EGFP, respectively. LO2 and HepG2 cells stably transfected with VASH2-targeting short hairpin RNA (shRNA) lentivirus for VASH2 knockdown (both 355 and 311 amino acid residues were downregulated) were designated as LO2-shVASH2 and HepG2-shVASH2, respectively. For knockdown, the shv2 construct, with ≥85% knockdown efficiency, was used for subsequent studies (Fig. 4). This shRNA sequences used for subsequent studies were: shVASH2, 5'-CCGGTTTGACTTTGAGGACTCTTACCTCGAGGTAAGAGTCCTCAAAGTAAATTTTTG-3'; shScrambled, 5'-CCGGCCTAAGGTTAAGTCGCCCTCGCTCGAGCGAGGGCGACTTAACCTTAGGTTTTTG-3' (4). LO2 and HepG2 cells stably transfected with scrambled shRNA lentivirus as controls were designated as LO2-shcont and HepG2-shcont, respectively.

Immunofluorescence. HepG2 cell line was arrayed in a 24-well plate (Corning Inc., NY, USA) and immunofluorescence was performed as previously described (11,12). The polyclonal antibodies were diluted as previously described (10). Mouse-anti-DDK antibody was purchased from Abmart (Arlington, MA, USA). The secondary antibody used was the goat anti-rabbit IgG-dylight 593 (Sigma-Aldrich, St. Louis, MO, USA). The nucleus dye, 10 μg/ml DAPI (Sigma-Aldrich) was diluted in PBS. The cells were then observed under a fluorescence microscope (Olympus, Tokyo, Japan).

Bromodeoxyuridine (BrdU) cell proliferation assay. Cultured cells ($1x10^5$/well) were plated in 96-well plates. Cell proliferation at 24, 48 and 72 h was evaluated using a BrdU Cell Proliferation Assay kit (cat. no. 11647229001; Roche Applied Science, Mannheim, Germany) according to the manufacturer's instructions. The cell proliferation rate was determined by measuring the absorbance at 492 nm using a computer-controlled microplate reader (Multiskan FC; Thermo Scientific, Waltham, MA, USA) (13).

Fluorescence-activated cell sorting analysis. Cells were collected, washed with 300 μl cold phosphate-buffered saline and precipitated with 3 ml cold 75% ethanol. Cells to be used for fluorescence-activated cell sorting (FACS) were stored at -20˚C in 75% ethanol for 16 h, stained with propidium iodide for 30 min at 37˚C and the DNA content analyzed using a FACS Calibur unit (BD Biosciences, Allschwil, Switzerland) (14).

Nuclear extraction analysis and western blot analysis. Cytoplasmic and nuclear protein samples were isolated using a Nuclear Extraction kit 2900 (Millipore, Billerica, MA, USA) according to the manufacturer's instructions. Total cell lysates were prepared using a radioimmunoprecipitation assay buffer

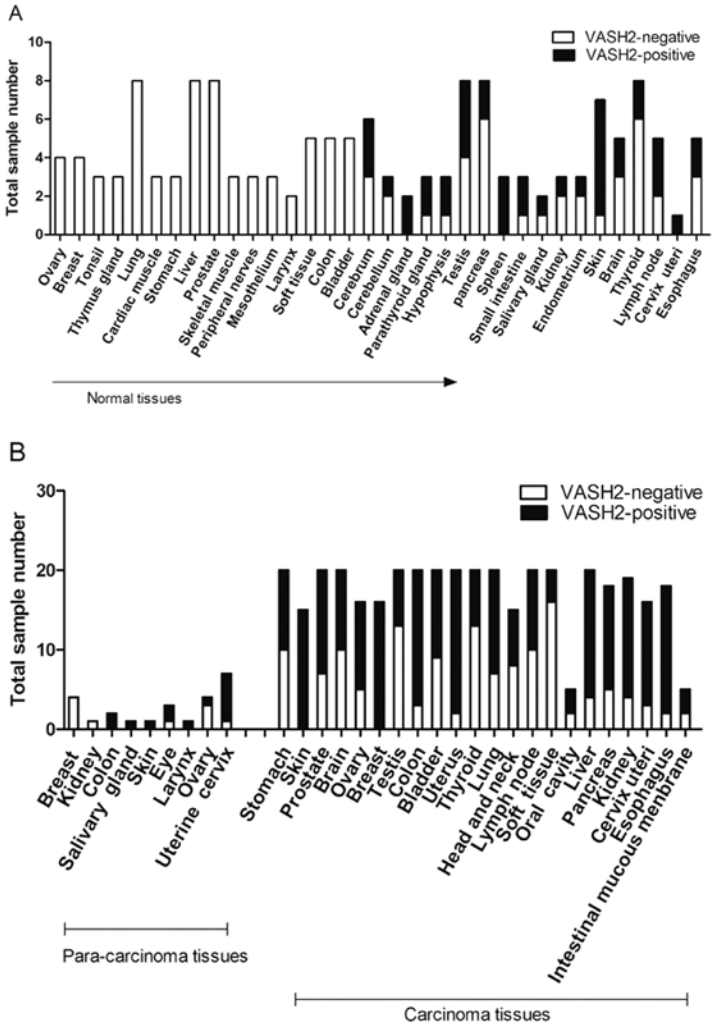

Figure 1. Nuclear VASH2 expression in normal tissues and cancer tissues from various organs. (A) Nuclear VASH2 expression in normal tissues. There was no nuclear VASH2 staining in 16 normal tissues; histologically, there were a variety of mature tissue elements. There was an extremely low VASH2 expression in the proliferative area in 18 normal tissues. (B) Positive nuclear VASH2 expression in seven tumor-adjacent tissues; 22 malignant tumors with strongly uncontrolled self-renewal ability were nuclear VASH2-positive. VASH2, vasohibin-2.

(Beyotime, Nantong, China). Protein quantities of 40 μg/lane for LO2 cell synchronization were used for western blotting. Polyvinylidene difluoride membranes (Millipore) were blocked with 5% non-fat dried milk and incubated overnight at 4˚C with the appropriate primary antibodies. The rabbit anti-human VASH2 polyclonal antibody was used as reported previously described (10).

Statistical analysis. A two-sample t-test was performed to compare the mean IHC scores for nuclear VASH2 between benign and malignant tissues overall and in a specific organ/system. The Spearman's rank correlation test was used for correlation analysis between nuclear VASH2 and Ki-67. Cell cycle group comparison was performed using an independent sample t-test. We used the Student-Newman-Keuls test for inequality of unpaired multiple data sets to determine significant differences in BrdU absorbance in the 24-, 48- and 72-h groups.

Results

Screening of nuclear VASH2 expression in normal and tumor tissues. We used a tissue microarray chip (547 specimens) to identify expression trends to analyze nuclear VASH2 expression in human normal and tumor tissues. Based on the tissue microarray, there were 34 normal human tissue (140 specimens), 22 primary malignant tumor (383 specimens) and 9 tumor-adjacent normal tissue types (24 specimens). There was positive VASH2 staining in 27.1% (38/140) of the normal human tissues. The 16 VASH2-negative normal mature human tissue types were derived from the ovary, breast, tonsil, thymus gland, lung, cardiac muscle, stomach, liver, prostate, skeletal muscle, peripheral nerves, mesothelium, larynx, soft tissue, colon and bladder (Fig. 1A). VASH2 expression localized to the nucleus was detected in the remaining 18 tissue types, including the cerebrum (3/6), cerebellum (1/3), adrenal gland (2/2), parathyroid gland (2/3), hypophysis (2/3), testis (4/8), pancreas (2/8), spleen (3/3), small intestine (2/3), salivary gland (1/2), kidney (1/3), endometrium (1/3), skin (6/7), brain (2/5), thyroid (2/8), lymph node (2/5), cervix uteri (1/1) and esophagus (2/5) (Fig. 1A).

In the normal tissue specimens, there was usually an absence of cell proliferation in the nuclear VASH2-negative tissues (Fig. 2), whereas there was usually strong cell and nuclear division and cytokinesis in nuclear VASH2-positive

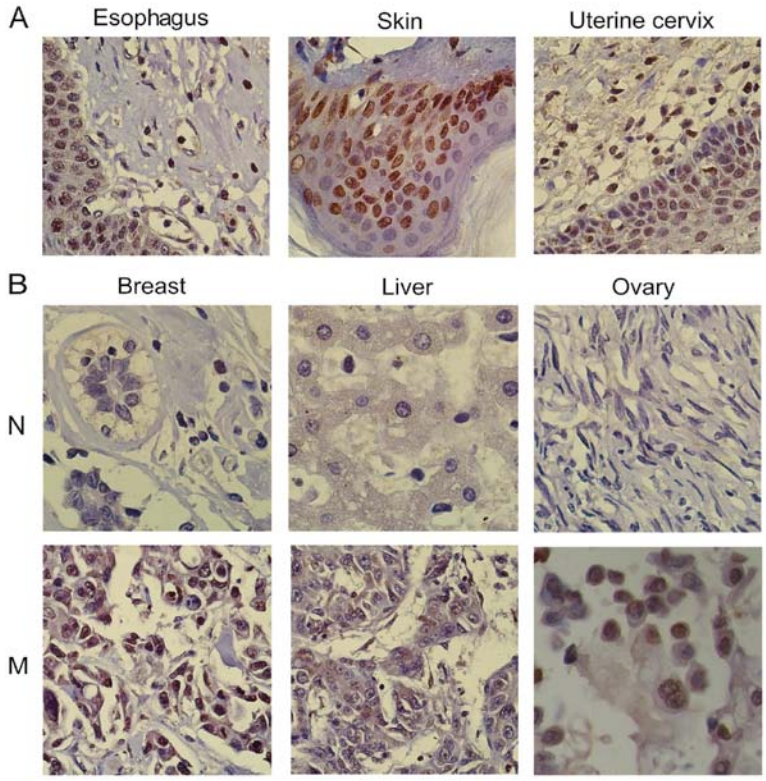

Figure 2. IHC analysis of nuclear VASH2 expression in normal tissues and common human cancers. (A) Strongly positive nuclear VASH2 staining expression in the proliferative basal and parabasal layers of normal esophagus, skin and uterine cervix. (B) Nuclear VASH2-negative mature human normal breast tissue (N), while invasive ductal carcinoma of breast with high nuclear VASH2 expression (M). Mature liver tissue showing no nuclear VASH2 staining (N), while positive nuclear VASH2 staining in many hepatocarcinoma cells (M). No nuclear VASH2 expression in normal ovary (N) but strongly positive nuclear VASH2 staining in the nuclei of serous cystadenocarcinoma (M). Magnification, x400. N, normal; M, malignant; IHC, immunohistochemistry; VASH2, vasohibin-2.

tissues (Fig. 2). There was deep nuclear VASH2 staining in the basal and parabasal layer cells of normal skin, small intestine, cervix uteri and esophageal tissues and these tissues were accompanied by numerous mitotic figures (Fig. 2).

We observed positive nuclear VASH2 staining in seven tumor-adjacent normal tissue types, including colon (2/2), salivary gland (1/1), skin (1/1), eye (2/3), larynx (1/1), ovary (1/4) and uterine cervix (6/7) (Fig. 1B). The nuclear VASH2-positive proportion in primary malignant tumor tissue specimens (22 tumor types) (64.8%, 248/383) (Fig. 1) was significantly higher than that of normal tissues (27.1%, 38/140, $P<0.001$). In addition, the tumor tissues were characterized by high proliferation capability (20). A high VASH2 expression in the nucleus was correlated with strong cytokinesis; dark, pathological mitotic figures; large, deeply stained nuclei and a high nucleo-cytoplasmic ratio (Fig. 2). However, these results need to be reconfirmed with an increasing size in these tissues. Table I showed significant differences in the expression levels of nuclear VASH2 between benign and malignant changes in different tissues. Based on these observations, it was determined that nuclear VASH2 may correlate with cell proliferation.

Positive correlation of nuclear VASH2 with cell proliferation. To examine the relationship between nuclear VASH2 and cell proliferation, we investigated nuclear VASH2 expression in proliferative normal squamous epithelium, adjacent non-tumor liver and hepatocarcinoma tissues. Proliferation was assessed by detecting Ki-67, which is widely used as a proliferation marker in histopathology (15-18). The Ki-67- and nuclear VASH2-positive proportion were highest in the basal layer (75.00±5.00 and 85.00±5.01%, respectively), intermediate in the parabasal layer (25.03±5.05 and 31.33±6.65%, respectively) and lowest in the superficial layer (2.10±1.15 and 4.00±1.00%, respectively) of normal squamous epithelium tissues (n=15, Fig. 3). We also calculated the Ki-67 and nuclear VASH2-positive proportion in the adjacent non-tumor liver tissues (n=15, 27.67±2.51 and 32.67±2.57%, respectively) and hepatocarcinoma tissues (n=15, 78.00±2.00 and 76.00±3.60%, respectively). The nuclear VASH2-positive proportion was positively correlated with the Ki-67-positive proportion in the basal ($r=0.80$, $P<0.05$), parabasal ($r=0.61$, $P<0.05$), superficial layer ($r=0.99$, $P<0.05$), adjacent non-tumor ($r=0.59$, $P<0.05$) and malignant liver tissues ($r=0.88$, $P<0.05$, Fig. 3). These observations suggested that nuclear VASH2 was positively correlated with cell proliferation.

Generation and identification of stably transfected cells. Previous findings showed that full-length VASH2 promoted growth and angiogenesis in hepatocellular carcinoma (HCC) (4,8). Therefore, to investigate the functions of nuclear VASH2 in cell proliferation, we overexpressed and silenced nuclear VASH2 expression in LO2 and HepG2 cells. We constructed VASH2 overexpression (311 amino acid residues) and VASH2-knockdown lentiviral constructs, infected HepG2 cells and selected stably infected cells for further study. We confirmed expression levels using western blot analysis (Fig. 4). The stable cells of LO2 were treated in the same manner as HepG2.

Table I. Statistically significant nuclear VASH2 expression levels (IHC score) between benign and malignant changes in different organs/tissues.

Organ/tissue	No.	Benign changes (mean ± SD)	No.	Malignant changes (mean ± SD)	P-value
Stomach	3	0.006±0.0057	20	0.530±0.0523	0.017
Skin	7	0.772±0.0381	15	0.996±0.0058	0.001
Prostate	8	0.004±0.0062	20	0.657±0.0236	0.01
Brain	5	0.400±0.0187	20	0.624±0.0543	<0.001
Ovary	4	0.017±0.0095	16	0.710±0.0451	0.027
Breast	5	0.060±0.0790	16	0.988±0.0160	0.002
Colon	5	0.018±0.0081	20	0.847±0.0257	<0.001
Bladder	5	0.016±0.0086	20	0.659±0.0628	0.006
Lung	8	0.006±0.0074	20	0.674±0.0366	0.041
Liver	8	0.012±0.0098	20	0.844±0.0306	0.006
Pancreas	8	0.003±0.0074	20	0.684±0.0422	0.032
Kidney	3	0.296±0.0251	20	0.836±0.0364	<0.001
Esophagus	5	0.456±0.1985	20	0.840±0.0380	0.001

VASH2, vasohibin-2; IHC, immunohistochemistry.

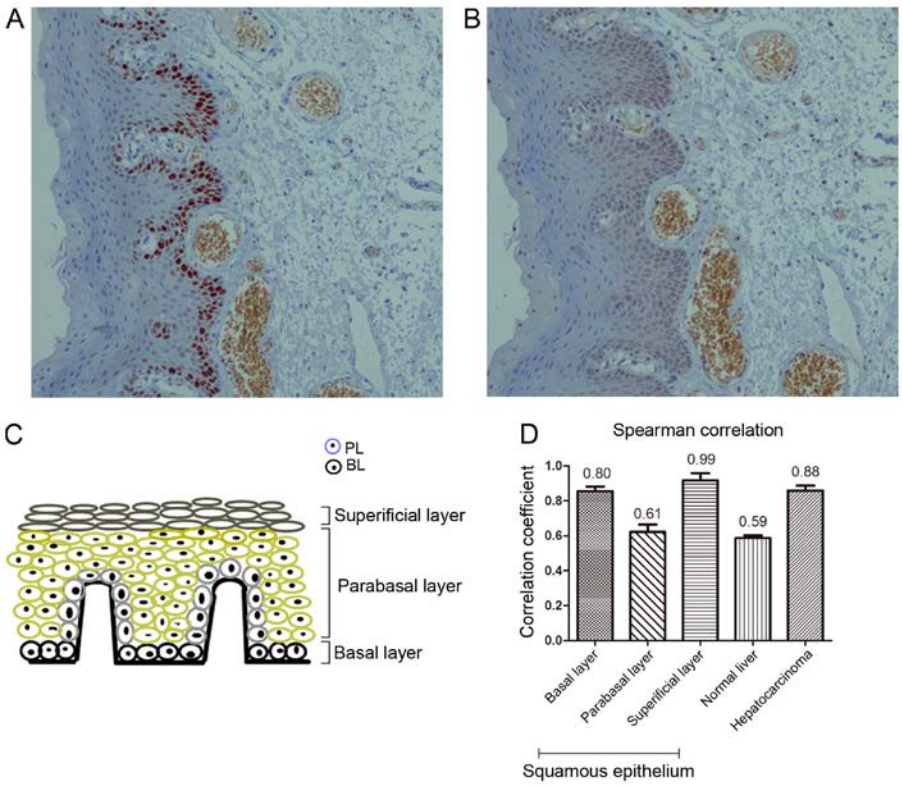

Figure 3. Nuclear VASH2 was positively correlated with cell proliferation. (A) Ki-67-positive cells were mainly present in the basal and parabasal layers in normal epithelium. (B) Nuclear VASH2-positive cells were restricted to the basal and parabasal layers in normal epithelium. (C) Diagrammatic illustration of classification of basal, parabasal and superficial layers in the epithelium. (D) Spearman correlation analysis determined that the nuclear VASH2-positive proportion was positively correlated with the Ki-67-positive proportion in the basal, parabasal and superficial layers and in adjacent non-tumor liver and malignant liver tissues. a and b, magnification, x200; PL, parabasal layer; BL, basal layer; VASH2, vasohibin-2.

To verify the localization of nuclear VASH2, immunofluorescence analysis was performed for the HepG2-VASH2 (transient overexpressed c-terminal V5 tag 311 and c-terminal DDK-tagged 355 amino acid residues VASH2). The HepG2-VASH2 (311 amino acid residues) nucleus was stained red while the cytoplasm was red in the HepG2-VASH2

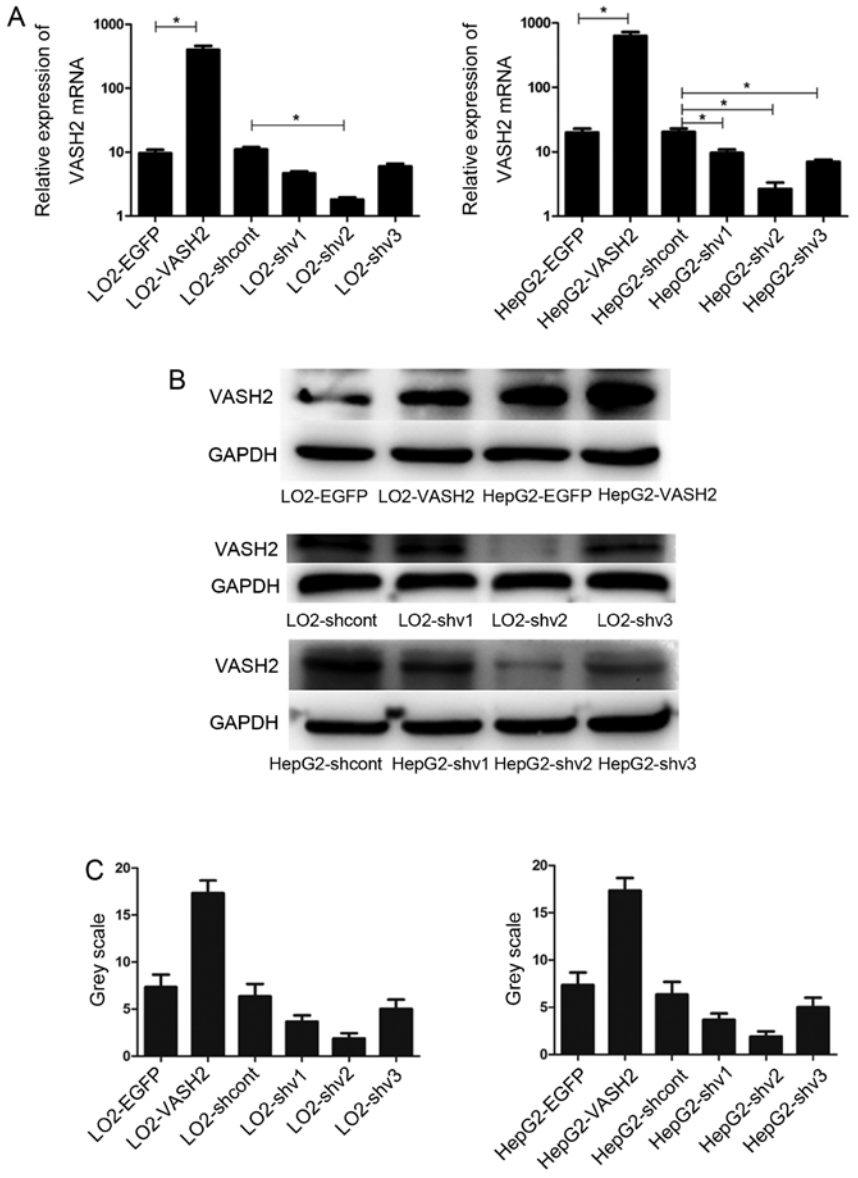

Figure 4. Generation and identification of stably transfected LO2 and HepG2 cells. (A) Measurement of VASH2 expression and knockdown using RT-qPCR. (B) Western blot analysis was used to confirm the efficiency of expression and knockdown. VASH2 indicates VASH2-overexpressing (34 kDa, 311 amino acid residues) LO2 and HepG2 cells; EGFP indicates LO2 and HepG2 cells transfected with a vector-expressing EGFP. The cells transduced with the three shRNAs and one control shRNA are designated as 'sh1', 'sh2', 'sh3' and 'shcont'. VASH2-overexpressed HepG2 cells showed a higher VASH2 expression than HepG2-EGFP cells, as well as LO2. Whereas VASH2-knockdown LO2 and HepG2 cells had an 80% decreased expression when compared with control-type LO2 and HepG2 cells. The shv2 construct, with ≥85% knockdown efficiency, was used for further studies. (*P<0.05 compared with the corresponding control group). The results were similar to those of RT-qPCR analysis. (C) Gray scale analysis of the western blot data. VASH2, vasohibin-2.

(355 amino acid residues) under the fluorescence microscope (Fig. 5).

Nuclear VASH2 promotes cell proliferation in vitro. We determined the proliferation ability of LO2-EGFP, LO2-VASH2, LO2-shcont, LO2-shVASH2, HepG2-EGFP, HepG2-VASH2, HepG2-shcont and HepG2-shVASH2 cells with BrdU analysis. The BrdU uptake assay revealed an increased DNA synthesis in LO2-VASH2 cells compared to LO2-EGFP cells (24-, 48-, 72-h post-plating; all P<0.001, Fig. 6); decreased DNA synthesis in LO2-shVASH2 cells after 48- and 72-h incubation (P<0.01 and P<0.001, respectively, vs. LO2-shcont cells, Fig. 6); markedly increased proliferation ability of HepG2-VASH2 cells compared to the control cells (24-, 48-, 72-h post-plating; all P<0.001 vs. HepG2-shVASH2 cells, Fig. 6); and decreased DNA synthesis in HepG2-shVASH2 cells after 48- and 72-h incubation (P<0.05 and P<0.001, respectively, vs. HepG2-shcont cells, Fig. 6). Compared to the control group, nuclear VASH2 overexpression in the LO2 and HepG2 cells resulted in significantly increased cell proliferation. VASH2 knockdown significantly reduced the proliferation of HepG2-shVASH2 compared to the HepG2-shcont and LO2 cells. These results indicated that nuclear VASH2 promotes cell proliferation. Considering BrdU incorporation can also be used to determine the S phase of the cell cycle (19), we hypothesized that nuclear VASH2 promotes cell proliferation by inducing cell cycle progression to the S phase.

Nuclear VASH2 induces cell cycle progression from G0/G1 to S phase. Compared with the control LO2-EGFP cells, there

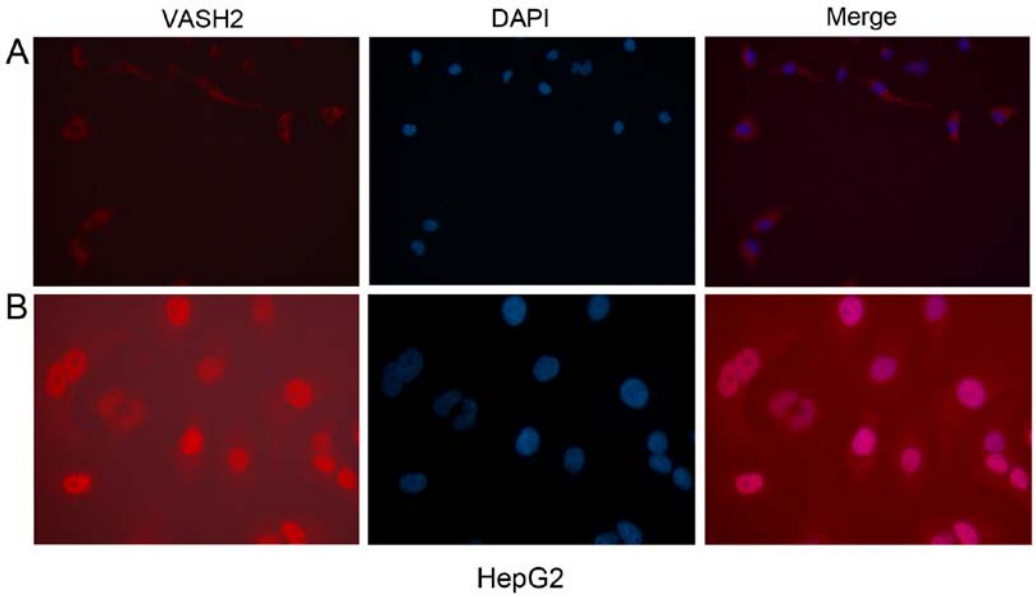

Figure 5. Intracellular localization of the VASH2 protein. (A) The 355 amino acid residues were mostly evident in the cytoplasm. (B) The 311 amino acid residues were present in the nucleus. HepG2-VASH2-Flag (355 amino acid residues); magnification, x200. HepG2-VASH2-Flag (311 amino acid residues); magnification, x400. VASH2, vasohibin-2.

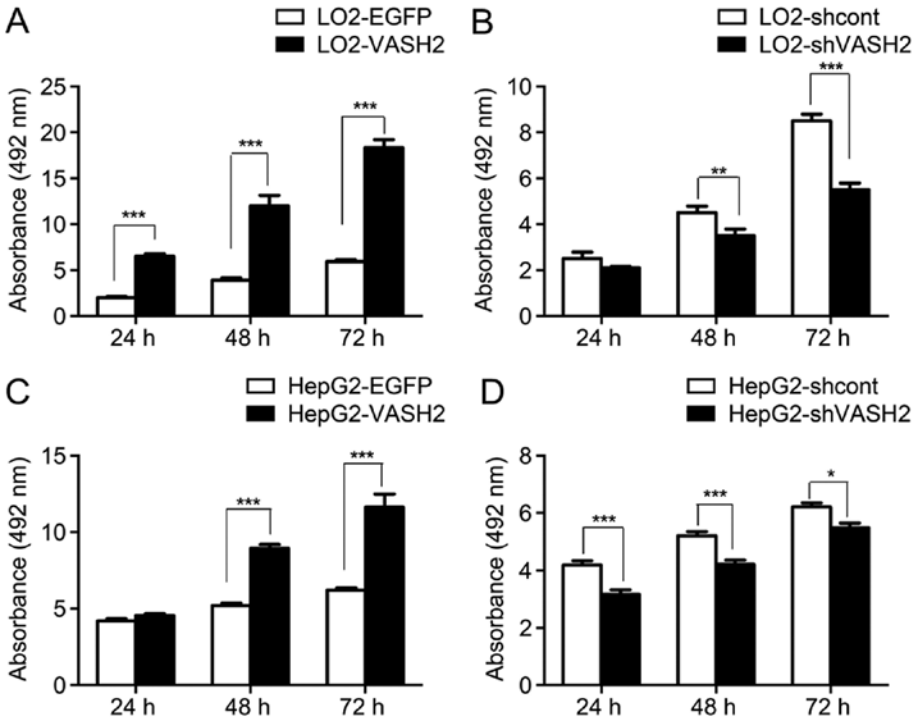

Figure 6. BrdU assay shows that nuclear VASH2 promotes cell proliferation. (A) BrdU uptake assay revealed increased DNA synthesis in LO2-VASH2 cells at 24, 48 and 72 h after seeding compared to the control LO2-EGFP cells (***P<0.001). (B) Decreased DNA synthesis in LO2-shVASH2 cells after 48- and 72-h incubation (**P<0.01, P<0.001 vs. LO2-shcont cells). (C) Markedly increased proliferation ability of HepG2-VASH2 cells compared to the control cells (***P<0.001 vs. the corresponding time for HepG2-shVASH2 cells). (D) Decreased DNA synthesis in HepG2-shVASH2 cells (*P<0.05, ***P<0.001 vs. HepG2-shcont cells). BrdU, bromodeoxyuridine; VASH2, vasohibin-2.

was an increased relative proportion of LO2-VASH2 cells in the S phase (30.44±4.26 vs. 52.56±5.32%, P<0.01, Fig. 7). Compared with the control LO2-shcont cells, there was an increased relative proportion of LO2-shVASH2 cells in the G_0/G_1 phase (60.05±3.38 vs. 75.88±12.22%, P<0.05, Fig. 7), but a reduced relative proportion of LO2-shVASH2 cells in the S phase (30.91±5.32 vs. 10.51±6.01%, P<0.01, Fig. 7). Compared with the control HepG2-EGFP cells, there was an increased relative proportion of HepG2-VASH2 cells in the S phase (30.05±10.92 vs. 45.13±5.22%, P<0.05, Fig. 7). Compared with the control HepG2-shcont cells, there was an increased relative proportion of HepG2-shVASH2 cells in the

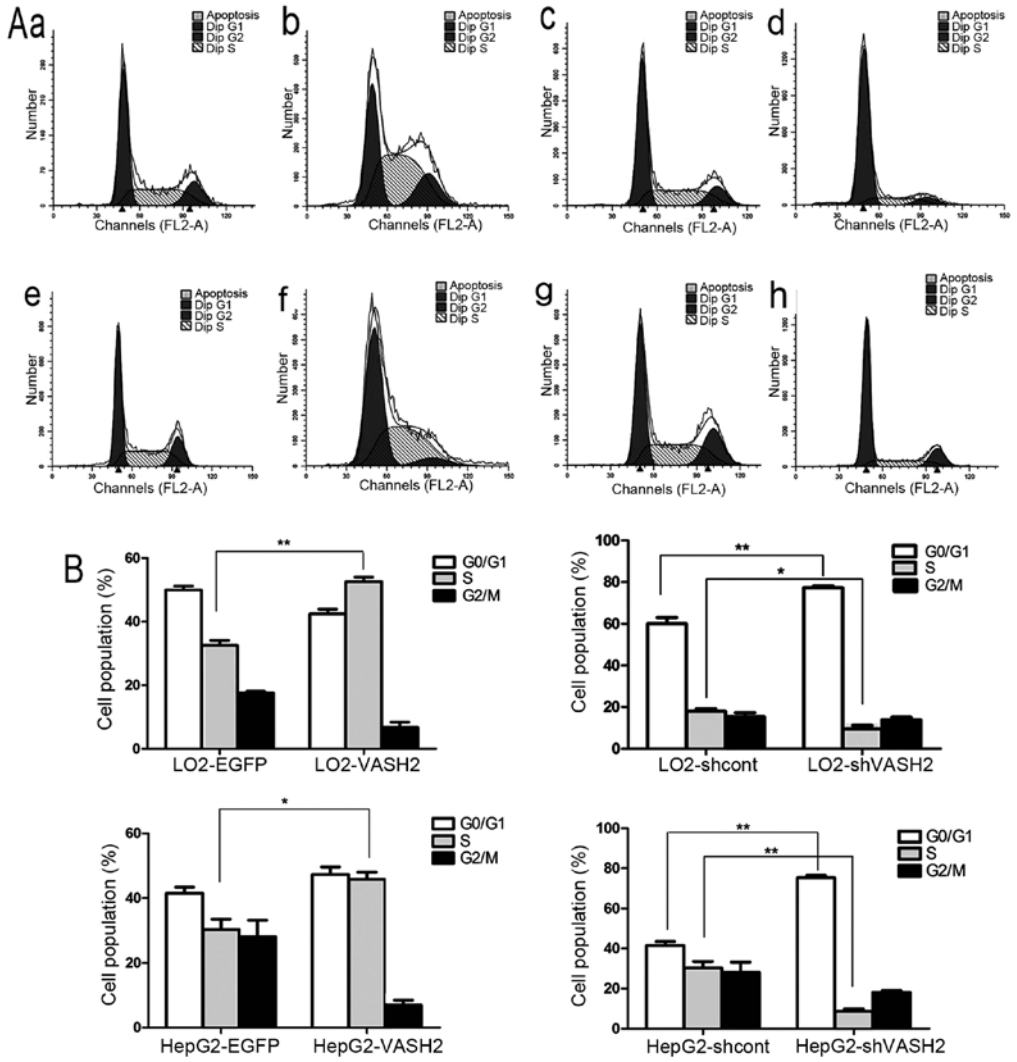

Figure 7. Nuclear VASH2 induces cell cycle progression from G_0/G_1 to S phase. (A) Flow cytometric analysis of DNA content. (A-a) LO2-EGFP control cells, (b) LO2-VASH2 cells (34 kDa, 311 amino acid residues), (c) LO2-shcont control cells, (d) LO2-shVASH2 cells, (A-e) HepG2-EGFP control cells, (A-f) HepG2-VASH2 cells (34 kDa, 311 amino acid residues), (A-g) HepG2-shcont cells, (A-h) HepG2-shVASH2 cells. (B) Increased relative proportion of LO2-VASH2 cells in the S phase compared to the control cells. Increased relative proportion of LO2-shVASH2 cells in the G_0/G_1 phase compared to LO2-shcont, but LO2-shVASH2 cells in the S phase were decreased. Increased relative proportion of HepG2-VASH2 cells in the S phase compared to the HepG2-EGFP cells; Increased relative proportion of HepG2-shVASH2 in the G_0/G_1 phase compared to the HepG2-shcont cells, although HepG2-shVASH2 cells in the S phase were decreased. *P<0.05, **P<0.01. VASH2, vasohibin-2.

G_0/G_1 phase (41.53±16.86 vs. 73.87±7.35%, P<0.01, Fig. 7), but a reduced relative proportion of HepG2-shVASH2 cells in the S phase (35.47±10.36 vs. 9.87±3.12%, P<0.01, Fig. 7). These results suggested that nuclear VASH2 induced cell cycle progression from G_0/G_1 to the S phase.

Discussion

Previously, it was reported that VASH2 is an angiogenesis factor associated with carcinoma angiogenesis and malignant transformation (1-6). VASH2 knockdown in cancer cells inhibits tumor growth and angiogenesis in an obvious manner (9). Besides that VASH2 also has shown a strong and extensive ability to promote tumor to EMT, increase the proportion of stem cells and inhibit apoptosis (7,8). We generated VASH2 polyclonal antibodies for immunoblotting and IHC (10). Based on its intracellular locations, we classified VASH2 into nuclear (with 311 amino acid residues) and cytoplasmic types (with 355 amino acid residues) (10). In the present study, we focused on nuclear VASH2, which, has not yet to be investigated so far.

We analyzed nuclear VASH2 levels in 547 tissue specimens, finding that proliferative cells in normal tissues tended to be nuclear VASH2-positive. Nuclear VASH2 was also expressed in most of the primary malignant tumor specimens, which are always highly proliferative (20). These observations indicated that nuclear VASH2 may be associated with cell proliferation.

Ki-67 is a good marker for detecting cell proliferation (18). We found that nuclear VASH2 staining was consistent with Ki-67 staining in normal squamous epithelial, adjacent non-tumor liver and hepatic cancer tissue. There was a high nuclear VASH2 expression in the basal and parabasal layers of the normal squamous epithelial tissue, where cell proliferation is high, whereas nuclear VASH2 was rarely expressed in the superior basal layer, where there is no mitosis or proliferation. In the adjacent non-tumor liver tissues, Ki-67 staining was consistent with that of nuclear VASH2. In malignant hepatic

tissues with a strong self-renewal ability, high Ki-67 staining was accompanied by a similarly high nuclear VASH2 staining. There was a significant positive correlation between nuclear VASH2 and Ki-67 staining, which indicates that nuclear VASH2 correlates positively with cell proliferation.

To identify the correlation between nuclear VASH2 and cell proliferation, we established nuclear VASH2 overexpression and knockdown cell models and used them in the BrdU proliferation test. Nuclear VASH2 overexpression in LO2 and HepG2 cells increased BrdU absorbance, while VASH2 knockdown decreased it, with only mitotic S-phase cells incorporating BrdU (21-22). Nuclear VASH2 increased the S-phase population and promoted cell proliferation. Based on these findings, we determine that nuclear VASH2 may promote cell progression by regulating the cell cycle.

To confirm this hypothesis, we analyzed the effect of nuclear VASH2 overexpression and knockdown on the cell cycle. Cell cycle analysis showed that VASH2 knockdown in LO2 and HepG2 cells increased the G_0/G_1 population and decreased the S-phase population and nuclear VASH2 overexpression promoted G_0/G_1 progression to the S phase. These results indicate that nuclear VASH2 regulates cell cycle progression from G_0/G_1 to the S phase.

An *in vivo* tumorigenicity experiment using HepG2 cells reported that VASH2 knockdown inhibited tumor growth significantly, while cytoplasmic VASH2 overexpression did not lead to greater tumor growth compared to the control cells (4). Using *in vitro* tetrazolium bromide proliferation assays, Xue *et al* (4) reported a significantly decreased proliferation rate of HepG2-shVASH2 (VASH2 knockdown) compared to HepG2 cells, while there were no differences between cytoplasmic VASH2-overexpressing HepG2-VASH2 (with 355 amino acid residues) and HepG2 cells. Cytoplasmic VASH2 did not promote cell proliferation in HepG2 cells *in vitro* and *in vivo*. The authors attributed this to the possibility that VASH2 expression in HepG2 cells is already relatively high and that the exogenous VASH2 overexpression did not alter its function (4). Both nuclear and cytoplasmic VASH2 were silenced when VASH2 was knocked down by shRNA, but the VASH2 overexpression detected was only that of cytoplasmic VASH2 in the study by Xue *et al* (4). In the present study, we confirmed that nuclear VASH2, encoding 311 amino acids, plays a definite role in promoting cell proliferation, where its overexpression (with 311 amino acid residues) induced cell proliferation significantly in HepG2 cells. Previously, we also determined that nuclear VASH2 is dominant while cytoplasmic VASH2 expression is very low in HepG2 cells (10). Our results are not in concordance with the those of Xue *et al* (4) who reported that VASH2 expression in HepG2 cells is already relatively high and that exogenous VASH2 overexpression has no effect on cell proliferation. We attribute the effect on HepG2 cell proliferation to nuclear VASH2, not cytoplasmic VASH2. However, we concede that cytoplasmic VASH2 may not promote cell proliferation in HepG2 cells.

Thus, to the best of our knowledge, the present study is the first to identify that nuclear VASH2 promotes cell proliferation. The present study improves the understanding of the functions of VASH2. However, the precise mechanism by which nuclear VASH2 regulates cell proliferation remains to be investigated.

Acknowledgements

The present study was partially supported by the National Natural Science Foundation of China (nos. 81272239, 81170336, 81172267 and 81372657), the Program for Development of Innovative Research Team in the First Affiliated Hospital of the Nanjing Medical University (Jiangsu, China), the Priority Academic Development Program of Jiangsu Higher Education Institutions (PAPD, JX10231801), the Special Research Fund for Public Welfare Industry of Health (201202007) and the Graduate Education Innovation Project of Jiangsu Province (JX22013230).

References

1. Shibuya T, Watanabe K, Yamashita H, Shimizu K, Miyashita H, Abe M, Moriya T, Ohta H, Sonoda H, Shimosegawa T, *et al:* Isolation and characterization of vasohibin-2 as a homologue of VEGF-inducible endothelium-derived angiogenesis inhibitor vasohibin. Arterioscler Thromb Vasc Biol 26: 1051-1057, 2006.
2. Suzuki Y, Kobayashi M, Miyashita H, Ohta H, Sonoda H and Sato Y: Isolation of a small vasohibin-binding protein (SVBP) and its role in vasohibin secretion. J Cell Sci 123: 3094-3101, 2010.
3. Sato Y: The vasohibin family: A novel family for angiogenesis regulation. J Biochem 153: 5-11, 2013.
4. Xue X, Gao W, Sun B, Xu Y, Han B, Wang F, Zhang Y, Sun J, Wei J, Lu Z, *et al*: Vasohibin 2 is transcriptionally activated and promotes angiogenesis in hepatocellular carcinoma. Oncogene 32: 1724-1734, 2013.
5. Takahashi Y, Koyanagi T, Suzuki Y, Saga Y, Kanomata N, Moriya T, Suzuki M and Sato Y: Vasohibin-2 expressed in human serous ovarian adenocarcinoma accelerates tumor growth by promoting angiogenesis. Mol Cancer Res 10: 1135-1146, 2012.
6. Koyanagi T, Saga Y, Takahashi Y, Suzuki Y, Suzuki M and Sato Y: Downregulation of vasohibin-2, a novel angiogenesis regulator, suppresses tumor growth by inhibiting angiogenesis in endometrial cancer cells. Oncol Lett 5: 1058-1062, 2013.
7. Tu M, Liu X, Han B, Ge Q, Li Z, Lu Z, Wei J, Song G, Cai B, Lv N, *et al*: Vasohibin-2 promotes proliferation in human breast cancer cells via upregulation of fibroblast growth factor-2 and growth/differentiation factor-15 expression. Mol Med Rep 10: 663-669, 2014.
8. Li Z, Tu M, Han B, Gu Y, Xue X, Sun J, Ge Q, Miao Y, Qian Z and Gao W: Vasohibin 2 decreases the cisplatin sensitivity of hepatocarcinoma cell line by downregulating p53. PLoS One 9: e90358, 2014.
9. Koyanagi T, Suzuki Y, Saga Y, Machida S, Takei Y, Fujiwara H, Suzuki M and Sato Y: In vivo delivery of siRNA targeting vasohibin-2 decreases tumor angiogenesis and suppresses tumor growth in ovarian cancer. Cancer Sci 104: 1705-1710, 2013.
10. Sun J, Tu M, Han B, Xue X, Zhang Y, Wei J, Chen J, Lu Z, An Y, Cai B, *et al*: Generation and characterization of rabbit polyclonal antibodies against Vasohibin-2 for determination of its intracellular localization. Int J Oncol 43: 255-261, 2013.
11. Tang S, Wang Y, Zhang D, Gao Y, Ma Y, Yin B, Sun J, Liu J and Zhang Y: Reprogramming donor cells with oocyte extracts improves in vitro development of nuclear transfer embryos. Anim Reprod Sci 115: 1-9, 2009.
12. Lin J, Lin X, Yang GH, Wang Y, Peng BW and Lin JY: Toxoplasma gondii: Expression of GRA1 gene in endoplasmic reticulum promotes both growth and adherence and modulates intracellular calcium release in macrophages. Exp Parasitol 125: 165-171, 2010.
13. Dolbeare F: Bromodeoxyuridine: A diagnostic tool in biology and medicine, part III. proliferation in normal, injured and diseased tissue, growth factors, differentiation, DNA replication sites and in situ hybridization. Histochem J 28: 531-575, 1996.
14. Danova M, Riccardi A and Mazzini G: Cell cycle-related proteins and flow cytometry. Haematologica 75: 252-264, 1990.
15. Scholzen T and Gerdes J: The Ki-67 protein: From the known and the unknown. J Cell Physiol 182: 311-322, 2000.
16. Cohen SM, Ohnishi T, Clark NM, He J and Arnold LL: Investigations of rodent urinary bladder carcinogens: Collection, processing, and evaluation of urine and bladders. Toxicol Pathol 35: 337-347, 2007.

17. Dwivedi N, Chandra S, Kashyap B, Raj V and Agarwal A: Suprabasal expression of Ki-67 as a marker for the severity of oral epithelial dysplasia and oral squamous cell carcinoma. Contemp Clin Dent 4: 7-12, 2013.
18. Kramer E, Herman O, Frand J, Leibou L, Schreiber L and Vaknine H: Ki67 as a biologic marker of basal cell carcinoma: A retrospective study. Isr Med Assoc J 16: 229-232, 2014.
19. Luo Y, Kleiboeker S, Deng X and Qiu J: Human parvovirus B19 infection causes cell cycle arrest of human erythroid progenitors at late S phase that favors viral DNA replication. J Virol 87: 12766-12775, 2013.
20. Robertson DS: The development of tumor cell characteristics. J Cell Physiol 229: 705-710, 2014.
21. Zhao P, Fu JL, Yao BY, Jia YR and Zhou ZC: S phase cell percentage normalized BrdU incorporation rate, a new parameter for determining S arrest. Biomed Environ Sci 27: 215-219, 2014.
22. Bahrami F, Morris DL, Rufener L and Pourgholami MH: Anticancer properties of novel aminoacetonitrile derivative monepantel (ADD 1566) in pre-clinical models of human ovarian cancer. Am J Cancer Res 4: 545-557, 2014.